# A liquid metal flume for free surface magnetohydrodynamic experiments

M. D. Nornberg, H. Ji, J. L. Peterson, and J. R. Rhoads
*Princeton Plasma Physics Laboratory, P.O. Box 451, Princeton, New Jersey 08543, USA*

(Received 7 June 2008; accepted 3 August 2008; published online 12 September 2008)

We present an experiment designed to study magnetohydrodynamic effects in free surface channel flow. The wide aspect ratio channel (the width to height ratio is about 15) is completely enclosed in an inert atmosphere to prevent oxidization of the liquid metal. A custom-designed pump reduces entrainment of oxygen, which was found to be a problem with standard centrifugal and gear pumps. Laser Doppler velocimetry experiments characterize velocity profiles of the flow. Various flow constraints mitigate secondary circulation and end effects on the flow. Measurements of the wave propagation characteristics in the liquid metal demonstrate the surfactant effect of surface oxides and the damping of fluctuations by a cross-channel magnetic field. © *2008 American Institute of Physics.* [DOI: 10.1063/1.2976109]

## I. INTRODUCTION

The stability of free surfaces in magnetohydrodynamics (MHD) plays a critical role in both heat and mass transfer problems and in turbulent mixing phenomena. The physical processes of free surfaces are important both in understanding astrophysical phenomena such as the enrichment of nova ejecta with heavy elements from white dwarfs and x-ray bursts due to accretion of plasma onto a neutron star surface[1] as well as in applications such as a liquid metal diverter in a fusion reactor design.[2,3] An experiment is presented in this paper that is designed to study free surface turbulent MHD flow using a liquid metal to provide the data critically needed to evaluate models for these open problems.

In a classical nova, the surface of a white dwarf accretes hydrogen rich material from a low-mass main-sequence companion star through an accretion disk. The accreted material eventually reaches thermonuclear temperatures and the hydrogen begins to burn, resulting in a tremendous explosion of material from the star. The ejecta from these outbursts have carbon, nitrogen, and oxygen (CNO) abundances greater than expected from nuclear processing during the hydrogen burn.[4] Several models for the CNO enrichment of nova ejecta have been proposed, including one that uses the same mechanism for ocean waves driven by wind shear.[5] The hydrogen and helium (H/He) plasma flowing onto the surface of the star from the surrounding accretion disk acts as a wind which drives gravity waves on the star surface. It is these breaking waves that dredge up the underlying layers of heavy elements.[1,6] Although the magnetic field of the white dwarf has been considered in the dynamics of the accretion disk during an outburst,[7] the damping of shearing instabilities by a magnetic field has not been adequately explored.[8,9]

Free surface dynamics also play an important role in the x-ray bursts from accreting neutron stars.[10] The surface of some neutron stars becomes so dense ($\rho > 10^9$ rmg/cm$^3$) that the H/He gas accreting onto the surface may crystallize into oceans.[11] These oceans can then go into thermonuclear runaway, creating a burn front which propagates across the neutron star surface. The locality of the burn front causes an asymmetry in the brightness of the neutron star which, due to the rapid rotation of the star, is observed as an x-ray burst oscillation with the burn front propagation velocity governing the burst dynamics.[12] Although the wave and mixing dynamics of these oceans have been solved to determine the front propagation, the role of MHD effects, such as resistive damping and field generation, is still in question.[13]

The physics of free surface MHD has more practical importance in fusion research. A current problem in fusion reactor design is the selection of materials to be used for surfaces in close contact with the plasma. Conventional heat exchanger designs using water-cooled copper with an armor made of solid materials such as carbon, tungsten, and beryllium are unable to handle the expected heat flux of 10–30 MW/m$^2$ and are eroded by neutron bombardment.[14,15] Some proposed solutions to this problem involve replacing the solid surfaces with a flowing liquid.[16] Liquid metals are excellent thermal conductors, have been used in other heat exchange systems, e.g., in breeder reactors, and are proposed as a candidate for a liquid-wall diverter. A flowing surface would provide the ability to extract both heat and helium ashes from the plasma.[17] Furthermore, as the fusion reaction creates high-energy neutrons that damage the components in contact with the plasma, a liquid metal first wall would be self-repairing, thereby reducing the maintenance required on the vessel.

The extent to which the liquid extracts heat and entrains particles is greatly dependent on the characteristics of the surface waves and the underlying turbulence. Heat flux measurements in turbulent channel flows with a nonconducting fluid suggest that the heat transport into the fluid is improved with increased wave amplitude and decreased wavelength on the surface.[18] Several liquid metal channel flow experiments at UCLA have been conducted as part of the APEX (Ref. 2) and ALPS (Ref. 3) programs with the intent of developing accurate analytical and numerical models of turbulent MHD open channel flow for the purposes of diverter design.[19–22]

Previous experiments exploring the basic properties of waves on a free surface conducting fluid have been con-

 

ducted in mercury with a similar channel configuration.[23] Alpher *et al.*[23] used an inclined 15 cm wide channel to obtain flow velocities up to 1 m/s with imposed vertical magnetic fields up to 4200 G to demonstrate the analogy between MHD channel flow and two-dimensional compressible flows. Their measurements included surface height and velocity measurements for varying boundary conditions created by a pair of electrodes at the side walls of the channel. They also examined wave damping in mercury at rest by driving standing waves, though their results are only qualitative. Ji *et al.*[24] performed precise measurements of the dispersion relation for gravity-capillary waves on a stationary pool of gallium with a streamwise magnetic field using a laser reflection diagnostic for measuring the wave number and damping rate of driven waves.

Section II of the paper describes design of the liquid metal flume used for the MHD experiments and the physical properties of the liquid metal. In Sec. III we report the results of using various techniques for shortening the transition to quasiuniform flow using honeycomb screens[25] and eliminating capillary disturbances due to entrance effects using a floating wave damper. The vertical velocity profile is modeled as a turbulent boundary layer using the Coles wake law[26] to fit measurements of the vertical velocity profile along the centerline of the channel. The friction velocity is computed as a parameter of the curve fitting and the fits reveal that the effective turbulent stress is reduced by damping surface waves from the channel entrance. The channel length required for uniform flow can thus be reduced.

Section IV details the experiments performed with the liquid metal. Surfactant effects due to oxides which form on the surface were quantified by driving waves with a fixed frequency with an oscillating paddle and measuring the wave number using the laser reflection diagnostic described by Ji *et al.*[24] The fluid depth and surface tension were then calculated as fit parameters for the gravity-capillary dispersion relation using the measured frequency and wave number. The results suggest that surface tension can vary greatly depending on the concentration of surface oxides.

The damping of surface fluctuations is examined for applied magnetic fields up to 2 kG to determine the role of a cross-channel magnetic field in shortening the development length in the channel. It is found that although the cross-channel magnetic field does not affect the propagation of streamwise waves, the turbulence giving rise to these waves is reduced, thereby reducing the source of the surface fluctuations.

## II. DESIGN OF THE CHANNEL AND LIQUID METAL TRANSFER SYSTEM

Several challenges in the design of the apparatus were met to achieve an experiment in which MHD effects on wave propagation could be distinguished from other effects. A fundamental constraint on the design was the limited volume of liquid metal available due to its high cost. As a result, the channel could not be made arbitrarily long to allow secondary circulation due to channel inlet effects to damp away. The distance required to achieve uniform flow (i.e., no downstream variation in the velocity profile) is known as the development length. Although the development length is well understood for pipe flow as a transition to the laminar Hagen–Poiseuille parabolic velocity profile via the spreading of viscous effects from the boundary layers at the walls,[27] the development length for open channel flow has only been given empirically.[28] Specifically, the role of gravity-capillary waves in developing channel flow has not been adequately explored.

TABLE I. Physical properties of $Ga^{67}In^{20.5}Sn^{12.5}$ alloy (Ref. 29).

| Property | Symbol | Units | Value |
|---|---|---|---|
| Melting point | $t_{mp}$ | °C | 10.5 |
| Density | $\rho$ | $kg/m^3$ | 6360 |
| Kinematic viscosity | $\nu$ | $m^2/s$ | $2.98\times10^{-7}$ |
| Conductivity | $\sigma$ | $(\Omega\ m)^{-1}$ | $3.1\times10^{6}$ |
| Surface tension | $T$ | N/m | 0.533 |

A problem peculiar to liquid metal experiments is that of oxide formation. The liquid metal used in the experiments is the eutectic alloy GaInSn whose physical properties are listed in Table I. It readily oxidizes in air to either $GaO_2$ which appears as a fine dark powder or the crystalline $Ga_2O_3$ on the surface of the eutectic.[30] Both oxides are less dense than the alloy ($\rho_{Ga_2O_3}=5880$ $kg/m^3$, $\rho_{GaO_2}=4770$ $kg/m^3$). Thus, they accumulate on the surface and form a thin film. The development of the film acts as a barrier to further oxidization. When the fluid is mixed by pumping, however, fresh eutectic is brought to the surface which can then entrain more oxygen from the air. Eventually enough gallium converts to gallium oxide, causing the other metals to precipitate out of the alloy as solids and the eutectic to gel. Efforts have been undertaken to perform the experiments in an inert atmosphere and to remove sources of oxygen entrainment to maintain a clean surface. In addition, a method of reduction by hydrochloric acid to remove oxides from the eutectic was developed and incorporated into the design of the liquid metal transfer system.

Even modest levels of oxidization of the eutectic, however, are problematic for surface wave experiments. The oxide film acts as a surfactant and can reduce the surface tension of a clean fluid.[23,31] Since we are interested in damping effects related to the applied magnetic field, effects due to concentration of impurities on the surface must be characterized first. A laser surface reflection technique described in Sec. IV is used to measure the surface tension of the liquid metal for varying levels of oxide contamination to quantify the effect.[24]

The channel, depicted in Fig. 1, is 106 cm long, 15.5 cm wide, and 2.5 cm tall and is mounted level. The channel walls are acrylic, as is the lid, which is mounted to the channel with an o-ring to make a gas-tight seal. Standard gear and centrifugal pumps were found to rapidly oxidize the GaInSn; so a custom-made helical screw pump was developed to drive fluid through the channel while minimizing the rapid mixing inherent to standard pumps. The pump is driven by a $\frac{1}{2}$ hp dc motor and the speed controlled by a dc motor amplifier with tachometer feedback. A double shaft seal is used to create a cavity filled with argon gas to prevent oxidization

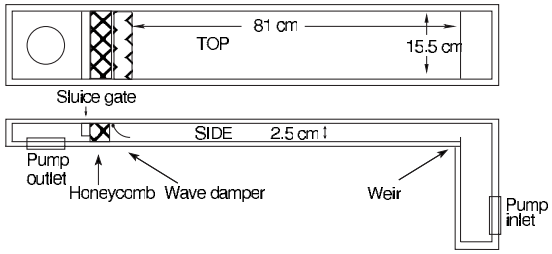


FIG. 1. A schematic of the channel used in the experiment showing the locations of the sluice gate, honeycomb, and wave damper in the channel.

in the event of seal failure. The pump is connected to the channel with polyvinyl chloride (PVC) pipe and flexible hose and is securely clamped to the floor to provide vibration isolation. Fluid enters a port on the bottom of the channel entrance and then passes through a sluice gate. In closed-channel flow such an obstacle would create a recirculation region,[32] but in open channel flow a hydraulic jump forms which may or may not have a region of recirculation. A 5 mm tall weir, a small submerged plastic plate, is placed at the end of the channel to ensure that the flow becomes supercritical before falling into the reservoir, thereby reducing end effects upstream.

The flow was characterized by visualization and velocimetry experiments to determine the appropriate method of minimizing entrance effects and establishing uniform flow. Several honeycombs of varying mesh size were placed after the gate but were found to be inadequate for minimizing the downstream secondary circulation. A plastic damper placed after the sluice to suppress wave generation from the channel entrance was found to be more effective. Typical flow speeds in the channel are 20 cm/s with flow heights of about 1 cm.

Once the velocimetry experiments were complete, the electromagnet was installed. The magnet flux path consists of a series of low-carbon hot-rolled steel plates. A coil of water-cooled oxygen-free high conductivity copper conductor is wound around the steel plates to provide the magnetic field. The magnet is constructed to withstand 7 kG with 6 kA coil current, although the present copper bus link configuration limits operation to 2.5 kA continuous operation.

The channel is drained and cleaned before introducing the GaInSn eutectic. For the liquid metal experiments, the channel is filled using the pneumatic transfer system shown in Fig. 2. Once the channel is sealed, the air inside is displaced with ultrahigh purity argon (99.999%). The remaining gas in the channel is circulated through a purifying filter to reduce oxygen content to less than 1 ppm.[33] The GaInSn alloy is then transferred to the channel by pressurizing an air bladder in the storage tank and venting the channel. Low-pressure check valves on the vent lines prevent air from re-entering the channel. After the GaInSn is transferred to the channel, the channel is kept at about 1 psi above atmospheric pressure to prevent oxidization through small residual leaks of air. Surface oxide contamination is removed by pumping the liquid metal through a treatment tank with a dilute HCl acid cover. The acid reacts with the oxides to form a salt, which is filtered from the alloy. Hydrogen released in the process is vented to prevent significant concentrations from accumulating.

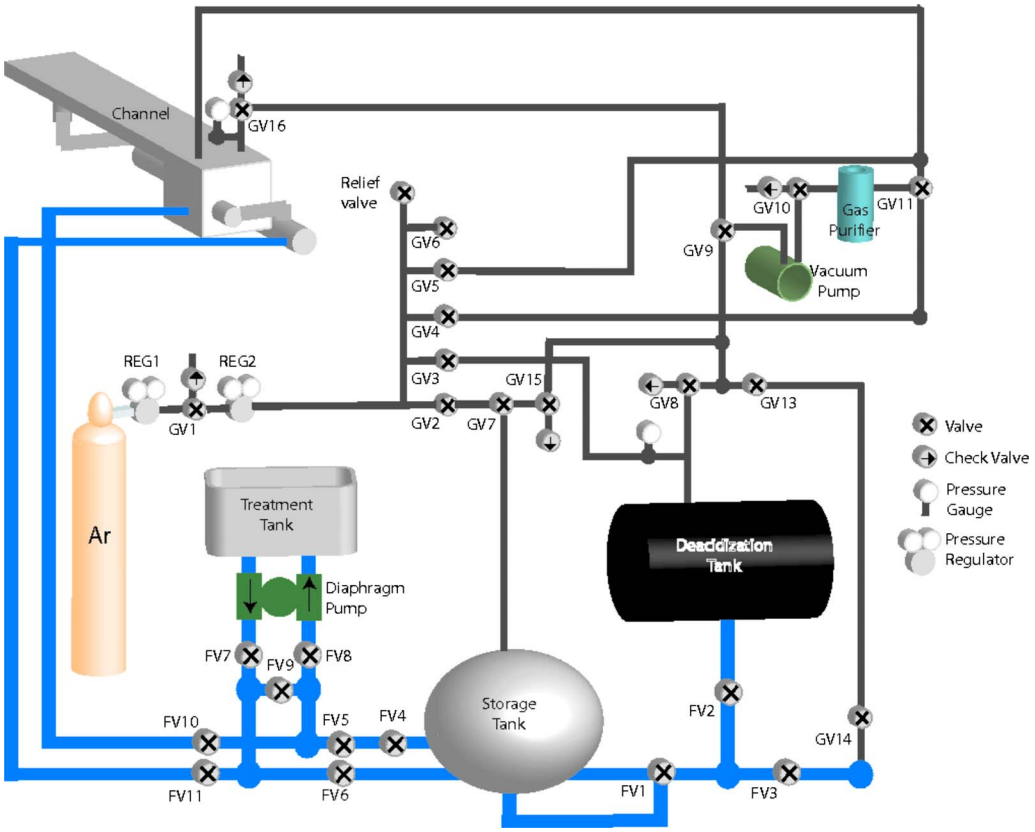


FIG. 2. (Color online) A schematic of the pneumatic transfer system used to convey the liquid metal alloy between a storage tank and the experiment.

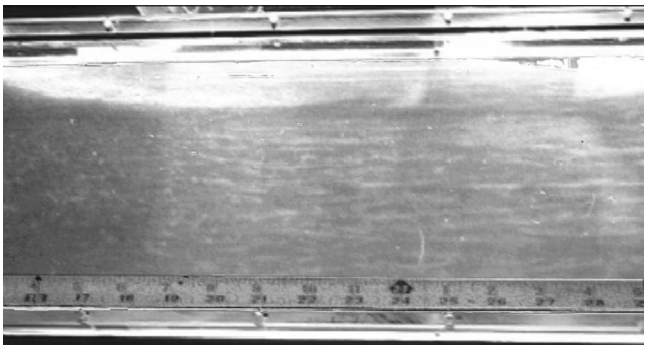

FIG. 3. Flow visualization of longitudinal vortices. The addition of a rheoscopic fluid reveals long streamwise vortices.

## III. VELOCIMETRY EXPERIMENTS WITH WATER

Kalliroscope, a rheoscopic fluid and standard visualization aid,[34] was added to the water to visualize the turbulent structures in the flow (Fig. 3). The Kalliroscope revealed longitudinal vortices throughout the channel which may play a role in the generation of surface waves and be a critical factor in heat and particle fluxes.[35]

Velocity data for water flowing through the channel were obtained using a 60 mW single-axis diode laser Doppler velocimetry (LDV) system made by Measurement Science Enterprise operated in backscatter mode.[36] LDV is noninvasive, requires no calibration, and has become a standard measurement technique for transparent fluids. The flow was seeded with 14 $\mu$m silvered glass beads with a specific gravity of 1.7 to serve as tracer particles. The measurement volume is about 3 mm along and 0.5 mm across the beam axis with a fringe spacing of 9.6 $\mu$m. The optical head was mounted to a computer-controlled traverse to provide precise relative positioning ($\pm 0.1$ mm) for each measurement. Velocity gradient broadening effects were minimized by orienting the laser to minimize the measurement volume along the direction of a scan. The laser entered the channel from the side wall for the streamwise scans in Fig. 4 and the vertical scans in Fig. 5. The sample time at each location was up to 2 min with sample rates varying between 1 and 30 Hz.

The flows studied in this paper have a characteristic surface speed of 20 cm/s (Re=7000). Nezu and Rodi's[28] criterion for uniform flow requires $x/h \geq 240/(1+2h/w)$ where $w$ is the channel width and $h$ is the flow height. For a wide channel where $h \ll w$, $x \geq 240h$. Surface gravity waves become unstable when the Froude number $\mathrm{Fr}=\nu/\sqrt{gh}$ exceeds unity, analogous to the Mach number in compressible flows.[37] The flows presented are subcritical with $\mathrm{Fr} \leq 0.6$. The data from Fig. 4 suggest that streamwise variation in the downstream velocity is sufficiently reduced within about 60 channel heights and that a quasiuniform approximation is appropriate. The vertical velocity profiles in Fig. 5 for flows with the gate and the gate with honeycomb both show a dip in the downstream velocity near the surface, indicating remnant secondary circulation as expected for a developing flow profile.[38] The absence of this velocity dip in the wave-damper flow suggests that secondary circulation has been minimized. It should be noted that the probability distribution functions of measurements near the surface are non-Gaussian with long tails extending to lower velocities. Hence, the calculated average value is slightly less than the most probable value.

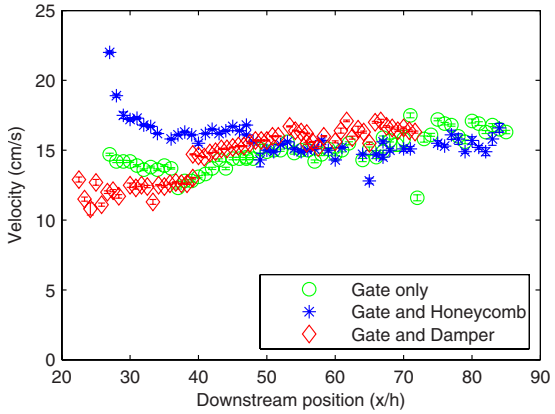


FIG. 4. (Color online) The downstream velocity profile for the three flows. Measurements were taken at the midheight of the flow along the center of the channel.

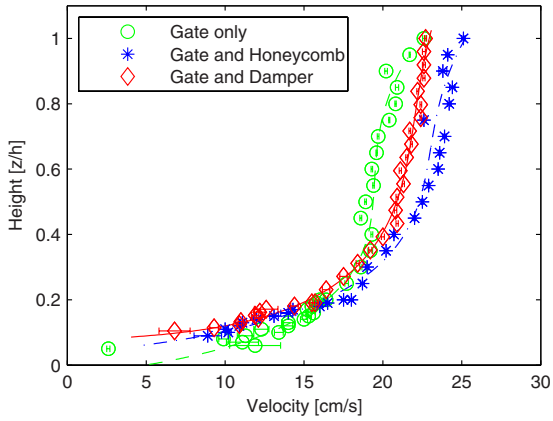


FIG. 5. (Color online) A plot of the vertical velocity profile in the developed flow at $x/h=78$ for the three different flows. The measurement height is normalized to the flow height.

Many treatments of the Reynolds stress typically break up the problem into an inner and an outer region with different scaling parameters to derive a law of the wall with different scaling parameters for the two regions. In the inner region where the Reynolds stress is weak, the friction velocity, defined as

$$v_* = \sqrt{\frac{\tau_w}{\rho}} = \sqrt{-\frac{h}{\rho}\frac{dP}{dx}}, \tag{1}$$

where $\tau_w$ is the wall stress, is used to scale $v_x(z)$. Similarly, $z^+ = z v_*/\nu$ is used for the length. In the outer region, the scaling follows a velocity defect law that scales on the global dimensions, i.e., the surface velocity $v_s$ and the boundary layer width $\delta$ in the case of developing flow or the flow height $h$ in the case of uniform flow.

Measurements of the Reynolds stress in channels indicate that the variation in the stress is roughly linear with distance from the wall in the outer region.[39,40] The effect of a linear Reynolds stress is to flatten the velocity profile. In fact, if the Reynolds stress is taken to be linear throughout the flow, the resulting velocity profile is constant with height.

TABLE II. Fit parameters for the Coles wake law in Fig. 5.

| Entrance condition | $h$ (cm) | $v_*$ (cm/s) | $A$ | $\Pi$ |
|---|---|---|---|---|
| Gate only | 1.15 | 5.349 | −14.65 | −0.5452 |
| Gate and honeycomb | 1.149 | 4.757 | −13.48 | −0.455 47 |
| Gate and damper | 1.151 | 2.365 | −7.737 | −0.35 |

At very large Reynolds numbers the viscous boundary layer that would be necessary to satisfy the no-slip condition at the channel bottom would be very thin; however, at the moderate Reynolds numbers for this experiment, the inner region should be resolved in the velocity measurements. In this case, the velocity profile must be derived from matching asymptotic expansions in the two scalings to produce a composite expansion.[41] The result is the addition of an empirical wake function $w(z/h)$ to the law of the wall

$$v_x^+(z) = \frac{1}{\kappa}\ln z^+ + A + w\left(\frac{z}{h}\right), \tag{2}$$

where Nezu[38] gave $w(z/h)=2\Pi/\kappa \sin^2(\pi z/2h)$ and $\kappa$ is the von Karman constant taken to be 0.41. The data for the vertical velocity profile are fitted to the composite log-wake function in Fig. 5 and the resulting fit parameters are given in Table II. The fits reveal that the friction velocity and wake parameters are minimized when the wave damper is placed after the sluice gate. These results suggest a relationship between the wave motion on the surface and the underlying turbulent boundary layer.[42] For the purposes of the design of the experiment, the important lesson is that surface waves play a strong role in propagating entrance effects downstream. By damping waves at the entrance, the secondary circulation in the developing flow is reduced, thereby leading to the establishment of uniform flow in a shorter development length.

## IV. LIQUID METAL SURFACE WAVE EXPERIMENTS

Preliminary experiments with the liquid metal involve measurement of the dispersion relation of gravity-capillary waves on the surface of the stationary liquid metal. The dispersion relation is given[24] by

$$\rho\omega^2 = (\rho g k + k^3 T + k j_y B_x)\frac{k}{K}\tanh(Kh), \tag{3}$$

where $\omega$ and $k$ are the wave frequency and (real) wave number, $g=9.8\ \mathrm{m/s^2}$, $h$ is the depth, $T$ is the surface tension of the fluid, $j_y$ is the cross-channel current density, $B_x$ is the streamwise magnetic field, and $K^2=k^2(1-i\sigma B_x^2/\rho\omega)$. An oscillating paddle driven by a Pasco Scientific SF-9324 mechanical wave driver powered by a Wavetek 188 function generator is used to drive single-frequency waves on the surface of the eutectic. A 4 mW He–Ne laser beam is split into seven diverging beams by a dot matrix diffraction grating. The seven laser beams are reflected off the surface of the liquid metal and projected onto a screen. A Watec LCL-902C charge coupled device (CCD) camera acquires images of the screen at a frame rate of 60 Hz, which are captured by a National Instruments PCI-1407 frame grabber. The images

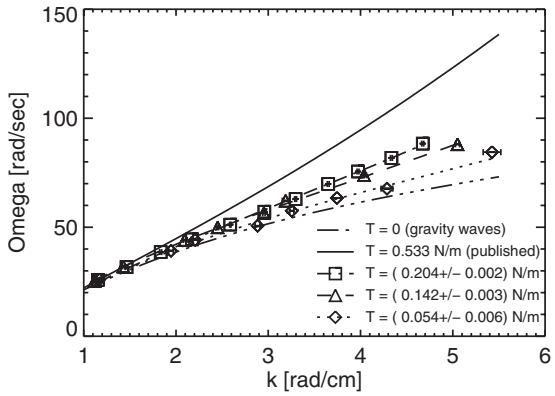


FIG. 6. Determination of surface tension from gravity-capillary wave dispersion measurements. The solid line shows the dispersion relation for the published surface tension of GaInSn. The dot-dashed line is the dispersion relation for pure gravity waves. Wave number and frequency measurements for visibly different surface conditions are shown: lustrous (squares), dull gray (triangles), and visible solids (diamonds).

are deinterlaced, so the camera is oriented to maximize the resolution in the direction of the driven waves. The position of each laser spot is calculated using an IDL routine that locates the centroid of the laser spot intensity in each image. Time series of each laser spot position are then constructed from the set of images. With proper calibration, the relative phase of the laser spot motion gives the wave number of the gravity-capillary wave on the surface. The frequency and phase of each of the laser spots are fit parameters to the sinusoidal waveforms from the spot position measurements and the wave number is calculated from a linear fit to the relative phase versus laser spot position. The measured $k$ and $\omega$ were then obtained from Eq. (3) using nonlinear least-squares fitting with $h$ and $T$ as free parameters. Figure 6 shows three cases with conditions ranging from a lustrous mirrorlike surface to one with visible solids. The surface tension measurements reveal that even with no visible oxides, the surface tension is a factor of 2 lower than that of the published value and can be considerably lower for visible surface oxidization.

When waves are driven on the surface, there is no change in the wave dispersion from an applied cross-channel magnetic field, as seen in Fig. 7. The natural surface fluctua-

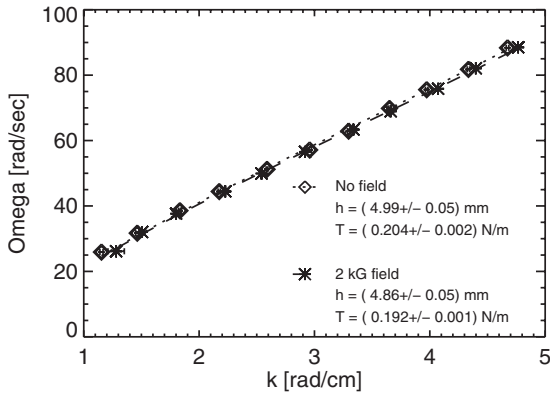


FIG. 7. Verification that a magnetic field has no effect on the dispersion of waves driven on a stationary pool of liquid metal when the field is perpendicular to the wave vector.

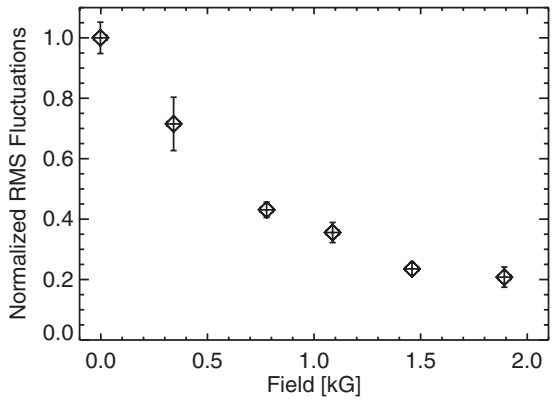


FIG. 8. Damping of cross-channel surface slope fluctuations with applied magnetic field. The fluctuation amplitudes, as quantified by the average standard deviation of the laser spot positions, are normalized to the fluctuations with no applied field. The CCD camera is oriented to maximize the resolution in the cross-channel direction.

tions due to the underlying turbulent boundary layer, however, display a gradual reduction in intensity with larger magnetic fields. A plot of the variation in the average standard deviation of the motion of the laser spots on the screen with applied magnetic field is shown in Fig. 8. This evidence would suggest that it is the underlying turbulent structures which are being damped by the magnetic field, resulting in a weaker drive for the surface fluctuations.

## V. SUMMARY

We have presented the design for a liquid metal flume to study free surface MHD in turbulent channel flow. Although the components of the channel and pump would not be compatible with other more reactive liquid metals such as lithium or sodium, the general principles of minimizing oxygen input and reducing entrainment through mixing are important design issues for any liquid metal experiment. The use of gas analysis may also prove useful in quantifying the oxygen in a system before introducing the liquid metal. Velocimetry measurements demonstrate that the flow is well approximated by the Coles wake law for a turbulent boundary layer, and that damping surface fluctuations near the entrance to the channel reduces secondary circulation. The effects of oxidization on surface tension were quantified by measuring the dispersion relation for driven waves on the surface of the liquid metal for varying degrees of oxidization. Although there is no effect on the propagation of driven waves when the magnetic field is perpendicular to the wave vector, we observed a damping of natural surface fluctuations due to turbulence suppression.

Experiments performed using this design will be supplemented by a linear stability analysis[43] and three-dimensional simulations[44] to aid in understanding the role of a magnetic field in turbulent free surface channel flow.

## ACKNOWLEDGMENTS

This work was funded by the Department of Energy under contract DE-AC02–76–CH039073. Special thanks go to R. Cutler for designing and building the pump, K. McMurty, A. Gill, and M. Burin for helping with the construction of the channel and diagnostics and for performing the LDV measurements, N. Morley for supplying materials for the magnet construction and design suggestions, R. Woolley for design of the magnet, R. Jensen for compiling information on gallium chemistry, L. Berzak who worked with R. Cava from the Princeton University Chemistry Department on GaInSn purification methods, and C. Weeks who we consulted on the HCl treatment.

[1] R. Rosner, A. Alexakis, Y. Young, J. Truran, and W. Hillebrandt, Astrophys. J. **562**, L177 (2001).
[2] M. Abdou, The APEX Team, A. Ying, N. Morley, K. Gulec, S. Smolentsev, M. Kotschenreuther, S. Malang, S. Zinkle, P. Fogarty, B. Nelson, R. Nygren, K. McCarthy, M. Z. Youssef, N. Ghoniem, D. Sze, C. Wong, M. Sawan, H. Khater, R. Woolley, R. Mattas, R. Moir, S. Sharafat, J. Brooks,A. Hassabein, D. Petti, M. Tillack, M. Ulrickson, and T. Uchimoto, Fusion Eng. Des. **54**, 181 (2001).
[3] J. Brooks, J. Allain, R. Bastasz, R. Doerner, T. Evans, A. Hassanein, R. Kaita, S. Luckhardt, R. Maingi, R. Majeski, N. B. Morley, M. Narula, T. Rognlien, D. Ruzic, R. Stubbers, M. Ulrickson, C. P. C. Wong, D. Whyte, and A. Ying, Fusion Sci. Technol. **47**, 669 (2005).
[4] J. Jose and M. Hernanz, J. Phys. G **34**, R431 (2007).
[5] J. Miles, J. Fluid Mech. **3**, 185 (1957).
[6] A. Alexakis, A. Calder, A. Heger, E. Brown, L. Dursi, J. Truran, R. Rosner, D. Lamb, F. Timmes, B. Fryxell, M. Zingale, P. M. Ricker, and K. Olson, Astrophys. J. **602**, 931 (2004).
[7] L. Angelini and F. Verbunt, Mon. Not. R. Astron. Soc. **238**, 697 (1989).
[8] J. M. Hameury, A. R. King, J. P. Lasota, and M. Livio, Mon. Not. R. Astron. Soc. **237**, 835 (1989).
[9] M. Livio, in *Magnetic Cataclysmic Variables*, Astronomical Society of the Pacific Conference Series Vol. 85, edited by D. A. H. Buckley and B. Warner (Astronomical Society of the Pacific, San Francisco, 1995), pp. 80–88.
[10] V. Urpin, Astron. Astrophys. **438**, 643 (2005).
[11] V. Urpin, Astron. Astrophys. **421**, L5 (2004).
[12] L. Bildsten, Astrophys. J. **438**, 852 (1995).
[13] A. Spitkovsky, Y. Levin, and G. Ushomirsky, Astrophys. J. **566**, 1018 (2002).
[14] H. Bolt, V. Barabash, G. Federici, J. Linke, A. Loarte, J. Roth, and K. Sato, J. Nucl. Mater. **307–311**, 43 (2002).
[15] R. Nygren, Fusion Eng. Des. **60**, 547 (2002).
[16] S. Mirnov, V. Dem'yanenko, and E. Murav'ev, J. Nucl. Mater. **196**, 45 (1992).
[17] A. Hassanein, J. Nucl. Mater. **307–311**, 1517 (2002).
[18] B. Freeze, S. Smolentsev, N. Morley, and M. Abdou, Int. J. Heat Mass Transfer **46**, 3765 (2003).
[19] N. Morley and J. Burris, Fusion Sci. Technol. **44**, 74-78 (2003).
[20] N. Morley, S. Smolentsev, R. Munipalli, M. Ni, D. Gao, and M. Abdou, Fusion Eng. Des. **72**, 3 (2004).
[21] A. Y. Ying, M. A. Abdou, N. Morley, T. Sketchley, R. Woolley, J. Burris, R. Kaita, P. Fogarty, H. Huang, X. Lao, M. Narula, S. Smolentsev, and M. Ulrickson, Fusion Eng. Des. **72**, 35 (2004).
[22] S. Smolentsev, N. Morley, B. Freeze, R. Miraghaie, J. Nave, S. Banerjee, A. Ying, and M. Abdou, Fusion Eng. Des. **72**, 63 (2004).
[23] R. Alpher, H. Hurwitz, Jr., R. Johnson, and D. White, Rev. Mod. Phys. **32**, 758 (1960).
[24] H. Ji, W. Fox, D. Pace, and H. L. Rappaport, Phys. Plasmas **12**, 012102 (2005).
[25] H. R. Bravo and J. W. Meinecke, Proceedings of the IAHR (IAHR, San Francisco, CA, 1997), pp. 723–728.
[26] D. Coles, J. Fluid Mech. **1**, 191 (1956).
[27] F. Durst, S. Ray, B. Ünsal, and O. A. Bayoumi, J. Fluids Eng. **127**, 1154 (2005).
[28] I. Nezu and W. Rodi, J. Hydraul. Eng. **112**, 335 (1986).
[29] N. B. Morley, J. Burris, L. C. Cadwallader, and M. D. Nornberg, Rev. Sci. Instrum. **79**, 056107 (2008).
[30] F. Gray, D. A. Kramer, and J. D. Bliss, *Kirk-Othmer Encyclopedia of Chemical Technology* (Wiley, New York, 2005), pp. 337–362.
[31] L. D. Landau and E. M. Lifshitz, *Fluid Mechanics* (Pergamon, Oxford, 1987).
[32] F. Durst and A. Rastogi, *Proceedings of the Symposium on Turbulent Shear Flows* (University Park, Pennsylvania, 1977), Vol. 1, pp. 18.1–18.9.

[33] The oxygen content was measured for a gas sample taken from another experiment connected to the transfer system by L. Ciebiera using a mass spectrometer.
[34] P. Matisse and M. Gorman, Phys. Fluids **27**, 759 (1984).
[35] S. Kumar, R. Gupta, and S. Banerjee, Phys. Fluids **10**, 437 (1998).
[36] H. E. Albrecht, *Laser Doppler and Phase Doppler Measurement Techniques* (Springer, Berlin, 2003).
[37] P. K. Kundu, *Fluid Mechanics* (Academic, San Diego, 1990).
[38] I. Nezu, J. Hydraul. Eng. **131**, 229 (2005).
[39] S. Yang, S. Tan, and S. Lim, J. Hydraul. Eng. **130**, 1179 (2004).
[40] B. Kironoto and W. Graf, Proc. Inst. Civ. Eng., Waters. Maritime Energ. **106**, 333 (1994).
[41] R. Panton, Appl. Mech. Rev. **58**, 1 (2005).
[42] R. Savelsberg and W. van de Water, Phys. Rev. Lett. **100**, 034501 (2008).
[43] D. Giannakis, P. Fischer, and R. Rosner, J. Comp. Physiol. (to be published).
[44] M. Narula, M. A. Abdou, A. Ying, N. B. Morley, M. Ni, R. Miraghaie, and J. Burris, Fusion Eng. Des. **81**, 1543 (2006).